VOL. 13, NO. 23, DECEMBER 2018 ISSN 1819-6608
ARPN Journal of Engineering and Applied Sciences

www.arpnjournals.com

C.F.D. ANALYSIS OFAIR-COOLEDHVAC CHILLER COMPRESSORS

Priyabrata Adhikary[1], Sumit Bandyopadhyay[2] and Asis Mazumdar[2]
[1]Department of Mechanical Engineering, New Horizon College of Engineering (V.T.U.), Bangalore, India
[2]S. W. R. E., Jadavpur University, Kolkata, India
E-Mail: priyabrata24@gmail.com

ABSTRACT

By using CFD analysis (FloEFD) and design services in HVAC industry, it's also reshaping the HVAC performance monitoring. The simulations account for all kinds of factors that influence fluid (refrigerant or air) flows, pressure and temperatures. They help create finely tuned designs even for installations in very confined spaces. CFD considers everything of HVACR from the direction of sunlight throughout the day, to structural materials, to the placement of air vents around furnishings. The goal is to figure out the best circulation solutions for the specific product or project space. Good agreement was found between the simulated results and standard manufacturer data for all three types of compressors studied in this research. To the best of the author's knowledge these novel approach for CFD analysis (FloEFD) of all air-cooled HVAC chiller compressors are absent in HVAC or fluid mechanics literature due to its assessment complexity.

Keywords: air-conditioning, refrigeration, chillers, HVAC, CFD.

1. INTRODUCTION

Building HVAC systems mean working with unique, custom-built interiors. There's no room for mistakes or costly trial and error.CFD enables HVAC industry to iron out nearly any air flow problem in advance. It gives us the ability to truly replicate the effects of an installation without having to build it first. Technology like this saves time and helps keep costs under control. With CFD, HVAC design engineer can design and plan customers' HVAC systems to the finest detail to avoid problems before they even occur.CFD is having a major impact on the way engineers design HVAC systems for their customers.

CFD analysis and design services by HVAC industry, is also reshaping the HVAC performance monitoring. The simulations account for all kinds of factors that influence fluid (refrigerant or air) flows and temperatures. They help create finely tuned designs even for installations in various spaces. CFD considers everything from the direction of sunlight throughout the day, to structural materials, to the placement of air vents around furnishings. The goal is to figure out the best circulation solutions for the specific product or project space.

2. MATERIALS AND METHODS

Fully embedded inside of DSS SOLIDWORKS, Flow Simulation (FloEFD) - CFD Tool is perfect for the HVAC engineer who needs flow analysis. There are usually no difficulties involved with CFD codes in simulating laminar flows which have clear unique solutions. However, direct simulations of turbulent flows as in HVAC considering fluid volume fluctuations are practically impossible because of the wide spectra of velocity fluctuations that would require extremely fine computation meshes to resolve them, long CPU times to simulate them and large computers to store the data produced. Hence, turbulent fluid flows as in HVAC are simulated today usually by considering their effect on the time-average fluid flow characteristics in the volume (finite volume method concept) being considered via semi-empirical models of turbulence that close the fundamental Navier-Stokes equations being solved (Wilcox, 1994). The two-equation k-ε empirical model for simulating turbulence effects in fluid flow (refrigerant gas or air) CFD simulation (Launder & Spalding, 1972 and Wilcox, 1994) is still widely used and considered reliable for most CFD simulations and it requires the minimum amount of additional information to calculate the flow field. In this the k-ε model is used with a range of additional empirical enhancements added to cover a wide range of industrial turbulent flow scenarios (such as shear flows, rotational flows etc.). Damping functions proposed by Lam and Bremhorst (1981) for better boundary layer profile fit when resolving boundary layers with computational meshes have been added (LB k-ε model).

In addition to turbulence modelling as in DSS Solid works Flow Simulation (FloEFD), when simulating fluid flows (refrigerant gas or air), it is also necessary to simulate fluid boundary layer effects near solid bodies or walls that can be difficult to resolve due to high velocity and temperature gradients across these near-wall layers. To solve the Navier-Stokes equations with a two-equation k-ε turbulence model without resolving the near-wall fluid boundary layer would require a very fine computational mesh, hence a "wall function" approach had been proposed by Launder and Spalding (1972, 1974) to reduce mesh sizes. According to this, the fluid wall frictional resistance and heat fluxes from the fluid to the wall are used to calculate the wall boundary conditions for solving the Navier-Stokes equations. Naturally, the main domain flow's physical properties will be those of the boundary layer's external boundary conditions.

In Flow Simulation (FloEFD) Van Driest's (1956) universal profiles are employed to describe turbulent boundary layers and two approaches (called "Two-Scale Wall Functions", 2SWF) have been devised to fit a fluid's boundary layer profile relative to the main flow's properties:

a) When the fluid mass centres of the near-wall mesh cells are located inside the boundary layer, i.e. the physical fluid flow boundary layer is thick,

b) When the fluid mass centres of the near-wall mesh cells are located outside the boundary layer, i.e. the physical fluid flow boundary layer is thin.

These two approaches allow it to overcome the traditional CFD code restriction of having to employ a very fine mesh density near the walls in the calculation domain and to use immersed boundary Cartesian meshes for all geometries (Kalitzin and Iaccarino, 2002) as in DSS Solidworks Flow Simulation (FloEFD).

3. THEORY AND CALCULATIONS

The flow of the refrigerant gas in the compressor is compressible and turbulent. In a Eulerian reference, the control equation of mass, momentum, energy [1-9] and other intensive properties applied to fluid flow in a control volume (CV) can be represented by a general transport equation:

$$\frac{d}{dt}\int_V \rho\Phi dV + \int_{\partial V} \rho\Phi U dA = \int_{\partial V} (\Gamma\Delta\Phi) dA + \int_V S dV$$

The solution domain of the control volume changes with time due to the movement of boundaries. The convective fluxes are calculated in these cases using relative velocity components at each cell face. The integral conservation equations presented in equation above must be modified when the control volumes' boundaries move in time. These modifications follow the application of the Leibnitz Rule, and the integral conservation equation with deforming boundaries becomes:

$$\frac{d}{dt}\int_V \rho\Phi dV + \int_{\partial V} \rho\Phi(U - U_j) dA = \int_{\partial V} (\Gamma\Delta\Phi) dA + \int_V S dV$$

U_j is the grid velocity which is independent of the fluid motion. It is controlled by the external program and reflected by controlling the grid displacement within a certain time. Its grid motion is described as follows. Here φ is scalar transported in CV, ρ is fluid density, Γ is diffusivity for the quantity φ, ∂V is surface enclosing CV, U is fluid velocity inside CV, V is volume of CV, S is source or sink of φ in the CV. DSS SOLIDWORKS Flow Simulation (FloEFD) - commercial CFD tool, is used here to save time-cost-effort.

For very complex systems the results are not very accurate, but CFD can still be very useful saving design engineer's time-cost-effort. Experimental validation verifies the codes to make sure that the numerical solutions are correct and compare the results (making a provision for measurement errors).Popular DSS Solid works Flow Simulation (FloEFD) or ANSYS-Fluent solver solves the Navier Stokes and conservation equations. The equations that we used are not closed, so we need to use Turbulence Modelling to close the equation set and then iterate towards a solution. We used what is called a Reynolds Averaged Navier Stokes (RANS) approach, (or we can use an Eddy Simulation technique which resolves the larger eddies in the flow and is only really required when you have separation or large re-circulating regions).

The most commonly used models are the RANS models due to their low cost in terms of compute power and run times. The Eddy Simulation methods can be quite mesh sensitive but will yield much better results for separated and re-circulating flow but takes much longer run times. There are different turbulence models available as mentioned below:

- Spalart-Allmaras Model;
- k-Ɛ (k-Epsilon) Model-widely used;
- k-ω (k-Omega) Model;
- v2-f Model;
- Reynold's Stress Model (RSM);
- Detached Eddy Simulation Model (DES);
- Large Eddy Simulation Model (LES) etc.

There are many possible reasons for the error or discrepancy between CFD calculation and experiment. Generally, we are modelling the problem as a steady flow that is symmetric about the axis, but experiments reveal that flow is neither steady nor symmetric. Furthermore, we are using a turbulence model. As discussed previously, all turbulence models are not universal, and may not be applicable to the present problem. A DES or LES simulation would be required to correctly model the unsteady turbulent eddies [10-20].

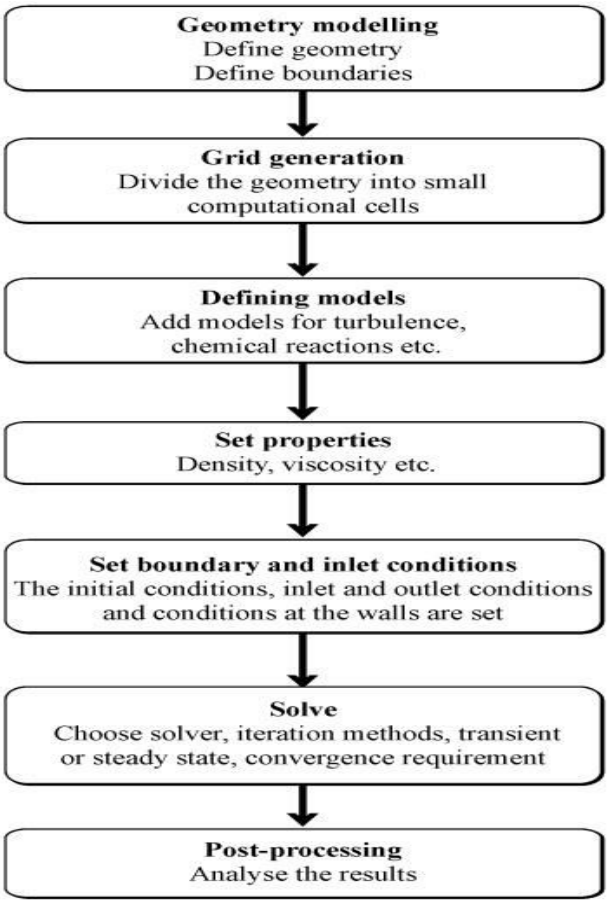

Figure-1. Steps for CFD analysis.

4. CASE STUDIES: RESULT AND DISCUSSIONS

High pressure rotary compressor

Geometrical parameters of the rotary compressor modelled here are: Displacement: 10.7 cc/rev; Pump chamber radius 21 mm; Roller diameter34 mm; Crankshaft eccentricity 3.9 mm; Pump chamber height 21.90 mm; Scanning clearance (θ = 270°) 0.01 mm at Speed 3600 rpm.

The operating conditions of the rotary compressor for R407C refrigerant are needed to maintain the evaporating and condensing temperatures at +10 °C and +55 °C. Both ambient temperature as well as outdoor design temperature are taken as +35.0 °C and compressor's rotational speed was operated at 3600 rpm. The pressure and temperature distribution of the rotary compressor are shown for R407Cgas. The pressure and temperature at upper and lower spaces changes alternatively. The upper and lower spaces are large enough and have no obvious pressure loss, but in the larger pressure difference between them, the pressure gradient can be observed obviously in the motor part. The difference of pressure between the upper and lower spaces of rotor would have axial load on the motor components. The difference pressure between the upper and lower spaces of rotor is very small, which is very low comparing to operating pressure. However, in practice, this difference pressure in the shell may be more due to uneven refrigerant gas-gap passage caused by vibration of crankshaft system as well as oil–gas two-phase flow in the narrow gas passage between the motor and the shell, which would lead to large refrigerant gas axial force of rotor components. Once the upward refrigerant gas force overcomes the weight of the rotor components, it may stimulate rotor components axial movement and cause vibration and noise, which often exists in practice.

In the present rotary compressor design and simulation, there is a segment difference left in the motor stator and rotor assembly. It is to impose an electromagnetic force on the rotor component in the gravity direction to ensure the resultant force of the rotor still to keep the same with gravity direction. Furthermore, the fluctuation of the gas force will not make rotor system produce axial movement. The simulated results were compared with standard manufacturer data. Good agreement was found between the simulated results and standard manufacturer data (not shown for the company privacy policy) for the rotary compressor [21-25].

Table-1. Properties of R-407C.

Physical Properties (R-407 C)		
Chemical Formula	$CH_2F_2/CHF_2CF_3/CH_2FCF_3$ (23/25/52% by weight)	
Molecular Weight	86.20	
Boiling Point at One Atmosphere	–43.56°C	(–46.40°F)
Critical Temperature, T_c	86.74°C 359.89 K	(188.13°F) (647.80°R)
Critical Pressure, P_c	4619.10 kPa (abs)	(669.95 psia)
Critical Density, D_c	527.30 kg/m³	(32.92 lb/ft³)
Critical Volume, V_c	0.00190 m³/kg	(0.0304 ft³/lb)

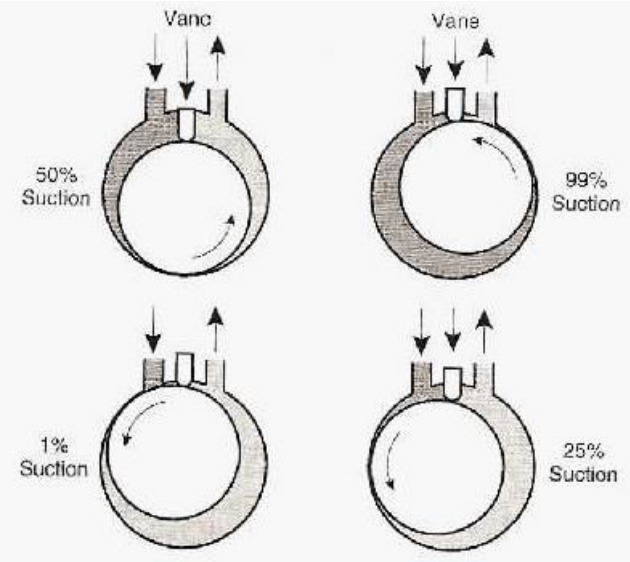

Figure-2. Rotary compressor operation.

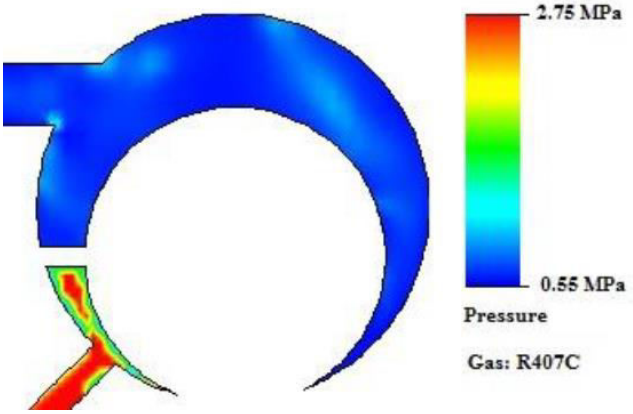

Figure-3. Rotary compressor simulation – Pressure.

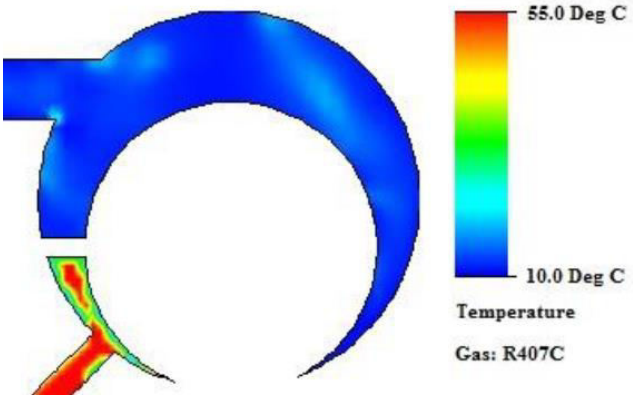

Figure-4. Rotary compressor simulation - Temperature.

Through CFD simulation of the flow field of domestic AC rotary compressor, some observations were obtained:

- Dynamic grid technique has been successfully used to simulate the transient flow mechanism of the domestic AC rotary compressor and could predict the performance of the compressor with a reasonable precision.
- Transverse refrigerant gas load of the roller accounts for a relatively large proportion in the rotor and for bearing support calculation itis not neglected.
- The pressure fluctuation obtained from refrigerant gas flow in the rotary compressor shell is main reason of the fluctuation of the axial force in rotor.
- The refrigerant gas resistance loss of the rotor is small relative to that of the roller.

High pressure scroll compressor

The operating conditions of the scroll compressor for R407C refrigerant are needed to maintain the evaporating and condensing temperatures at +10 °C and +55 °C. Both ambient temperature as well as outdoor design temperature is taken as 35.0 °C.

As shown below the pressure and temperature distribution for R407C refrigerant gas at crank angle of 0^{o}. As the suction port and passage are not symmetrical, the pressure distribution is not symmetrical in both suction chambers. These asymmetric phenomena are obvious in a pair of working chambers. In addition, the refrigerant gas pressure in the working chamber is almost homogeneous except at the meshing clearance. As the refrigerant gas leaks from the high-pressure chamber to the low-pressure chamber through the radial clearance, the pressure gradient is high in the near-flow domains of the radial clearance. Moreover, in the depth direction of the scroll vane, the pressure in one chamber is uniform. The pressure increases from the suction chamber to the discharge chamber. The simulated results were compared with standard manufacturer data. Good agreement was found between the simulated results and standard manufacturer data (not shown here for the company privacy policy) for the scroll compressor.

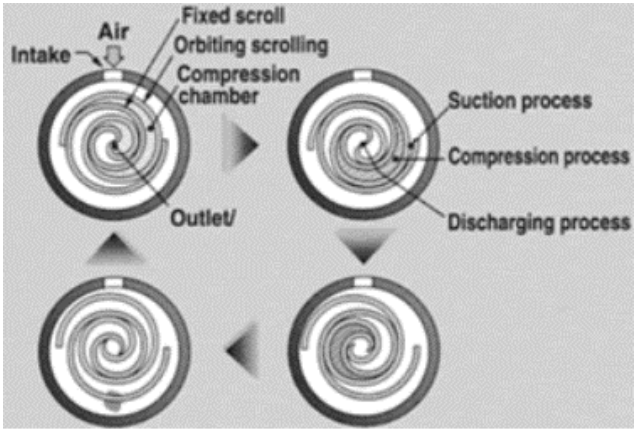

Figure-5. Scroll compressor operation.

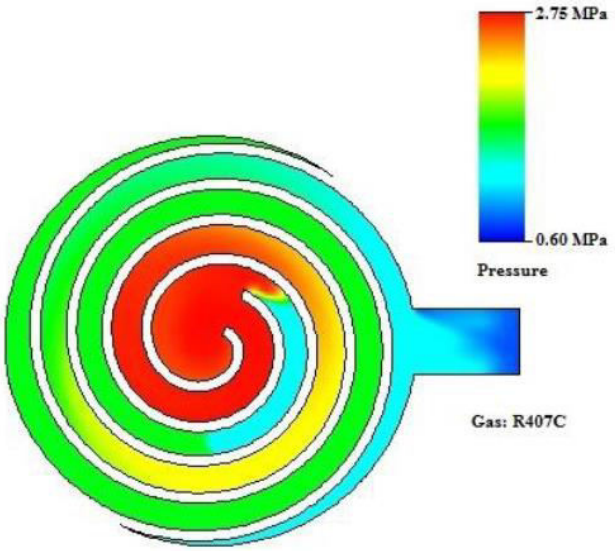

Figure-6. Scroll compressor simulation – Pressure.

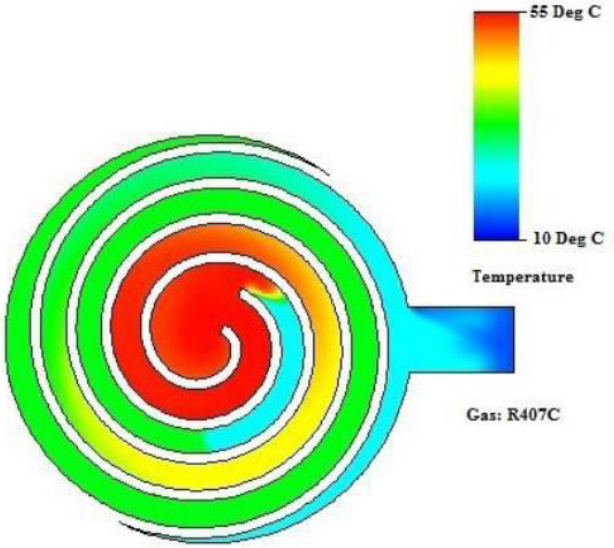

Figure-7. Scroll compressor simulation - Temperature.

The detailed physics of the transient flows of refrigerant gas inside the scroll compressor were analysed as mentioned below:

- The pressure was almost homogeneous in a working chamber but asymmetrical in few other chambers. The temperature and velocity distribution were inhomogeneous and asymmetrical owing to the leakage flow. The movement of the orbiting scroll contributed to the vortex formation in one chamber and restricted it in another one.

- The variation of the inlet mass flux was different from that of the suction volume with a crank angle. The outlet mass flux fluctuated when the terminal of the orbiting scroll intruded into the discharge port.

- At the radial clearance, the maximum velocity of the refrigerant gas is obtained; the pressure and temperature of the leakage fluid (refrigerant gas) decreased sharply and then recovered when it flowed through the radial clearance.

Low pressure screw compressor

The operating conditions of the screw compressor for low pressure refrigerant (R407C) are needed to maintain the evaporating and condensing temperatures at +5 °C and + 55 °C. Both ambient temperature as well as outdoor design temperature is taken as +35.0 °C.

The study was performed in a twin screw compressor with a male rotor radius of 63.4 mm. Initially, an attempt was made to generate a complete model for Key-frame re-meshing that included both radial and inter-lobe leakage gaps. A very fine grid was generated to capture the clearances. But, it was practically impossible to obtain a sufficient number of meshes and to perform this calculation. In the alternative attempt the radial clearances were excluded. The user defined nodal displacement method was then applied and the case was solved successfully. The simulated results were compared with standard manufacturer data. Good agreement was found between the simulated results and standard manufacturer data (not shown here for the company privacy policy) for the screw compressor.

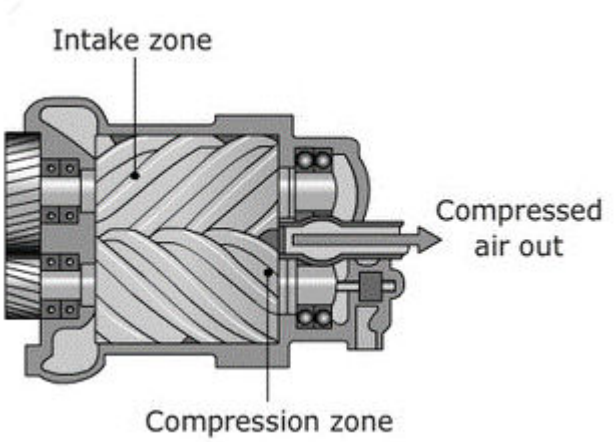

Figure-8. Screw compressor operation.

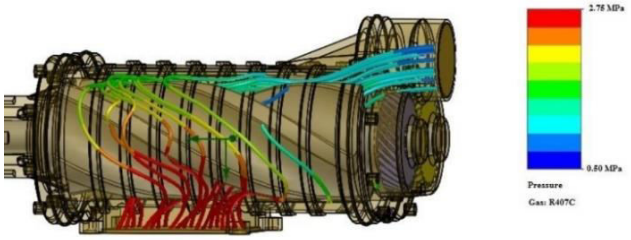

Figure-9. Screw compressor simulation - Pressure.

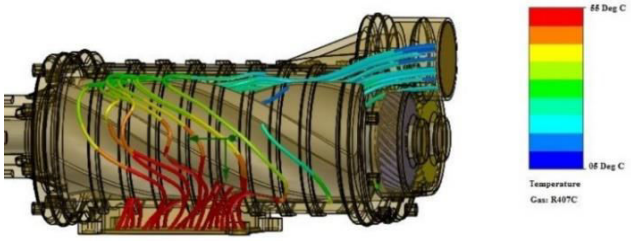

Figure-10. Screw compressor simulation - Pressure.

All attempts to solve refrigerant gas flow within a twin-screw chiller by use of Key-Frame Re-meshing failed, due to the complexity of the numerical mesh. However, by applying User Defined Nodal Displacement and using a customized grid generator, it was possible to demonstrate a suitable method for grid deformation solution in screw chiller CFD analysis with low-pressure refrigerant (R407C). Thus, for future work, it will be necessary to develop customized tools to generate CFD grids for complex screw machines.

5. CONCLUSIONS

Using smart computer modelling software, CFD tools enable HVAC system designers to realistically simulate fluid (refrigerant or air) flows within the product or project space in advance. As a result, we can accurately predict where problems such as drafts, high sound levels, or poor ventilation may occur. This allows us to optimise the HVAC system's design and ensure comfort and effectiveness - before actual installation work begins saving valuable time-cost-effort.

ACKNOWLEDGEMENT

The authors wish to thank S.W.R.E., Jadavpur University, Kolkata for the valuable technical support. The authors declare that there is no conflict of interests.

REFERENCES

[1] Adhikary P., Roy P.K. and Mazumdar A. 2013. Fuzzy Logic based optimum penstock design: Elastic Water column theory approach. ARPN Journal of Engineering and Applied Sciences. 8(7): 563-568

[2] Adhikary P., Roy P.K. and Mazumdar A. 2013. Optimum selection of Hydraulic Turbine Manufacturer for SHP: MCDA or MCDM Tools, IDOSI -WASJ. 28(7): 914-919

[3] Adhikary P., Roy P.K. and Mazumdar A. 2014. Multidimensional feasibility analysis of small hydropower project in India: a case study. ARPN Journal of Engineering and Applied Sciences. 9(1): 80-84

[4] Roy P.K., Adhikary P. and Mazumdar A. 2014. Preventive Maintenance Prioritization by Fuzzy Logic for Seamless Hydro Power Generation. J. Inst. Eng. India Ser. A. 95(2): 97-104

[5] Roy P.K., Adhikary P. and Mazumdar A. 2014. Turbine supplier selection for small hydro project: application of multi-criteria optimization technique, I.J.A.E.R. (R.I.P.). 10(5): 13109-13122

[6] Adhikary P., Roy P.K. and Mazumdar A. 2015. Maintenance contractor selection for small hydropower project: a fuzzy multi-criteria optimization technique approach, I.RE.M.E. 9(2): 174-181

[7] Adhikary P., Roy P.K. and Mazumdar A. 2015. Selection of small hydropower project site: a multi-criteria optimization technique approach. ARPN Journal of Engineering and Applied Sciences. 10(8): 3280-3285

[8] Adhikary P. Roy P.K. and Mazumdar A. 2015. Optimal renewable energy project selection: A multi-

criteria optimization technique approach. RIP-G.J.P.A.M. 11(5): 3319-3329

[9] Adhikary P., Roy P.K. and Mazumdar A. 2016. C.F.D. Analysis Of Micro Hydro Turbine Unit: A Case Study. ARPN Journal of Engineering and Applied Sciences. 11(7): 4346-4352

[10] Adhikary P., Roy P.K. and Mazumdar A. 2017. Application Of Artificial Intelligencein Energy Efficient H.V.A.C. System Design: A Case Study. ARPN Journal of Engineering and Applied Sciences. 12(21): 6154-6158

[11] P. Adhikary. 2018. Conference room AC system performance analysis: a case study, ICHVACR. (IEI - ISHRAE). pp. 117-120.

[12] P. Adhikary. 2018. Performance analysis of an office space HVAC system: a case study, ICHVACR. (IEI - ISHRAE). pp. 110-113.

[13] P. Adhikary, Data Centre cooling system performance analysis: a case study, ICHVACR 2018 (IEI - ISHRAE), pp. 106-109.

[14] P. Adhikary. 2018. CFD analysis of a Call Centre HVAC system: a case study, ICHVACR 2018 (IEI - ISHRAE). pp. 102-105.

[15] P. Adhikary. 2018. CFD analysis of dairy cold room: a case study, ICHVACR 2018 (IEI - ISHRAE). pp. 98-101.

[16] P. Adhikary. 2018. CFD analysis of HVAC Scroll Compressor performance - case study using two refrigerants (R407C and R410A), ICHVACR 2018 (IEI - ISHRAE). pp. 73-76.

[17] P. Adhikary. 2018. Performance analysis by CFD of Scroll Compressor using two high pressure refrigerants (R134A and R410A), ICHVACR 2018 (IEI - ISHRAE). pp. 69-72.

[18] P. Adhikary. 2018. CFD analysis of high pressure Scroll Compressor - comparison with two refrigerants (R134A and R407C), ICHVACR 2018 (IEI - ISHRAE). pp. 65-68.

[19] P. Adhikary. 2018. High pressure Rotary Compressor CFD analysis - Performance comparison of two R gases (R134A and R407C), ICHVACR 2018 (IEI - ISHRAE). pp. 61-64.

[20] P. Adhikary. 2018. CFD analysis of Twin Screw Compressor using low pressure refrigerants (HFD1234yp and R407C), ICHVACR 2018 (IEI - ISHRAE). pp. 55-58.

[21] P. Adhikary. 2018. CFD analysis of low-pressure Screw Compressor using two refrigerants (HFD1234yp and R123), ICHVACR 2018 (IEI - ISHRAE). pp. 51-54.

[22] P. Adhikary. 2018. Performance analysis of HVAC Twin Screw Compressor: study with two different refrigerants (R123 and R407C), ICHVACR 2018 (IEI - ISHRAE). pp. 47-50.

[23] P. Adhikary. 2018. Rotary Compressor performance analysis by CFD using two high pressure refrigerants (R134A and R410A), ICHVACR 2018 (IEI - ISHRAE). pp. 43-46.

[24] P. Adhikary. 2018. Rotary Compressor performance analysis comparison using two high pressure refrigerants (R410A and R407C), ICHVACR 2018 (IEI - ISHRAE). pp. 39-42.

[25] P. Adhikary. 2018. Modelling and analysis of Cooling Tower Pump - a case study, ICHVACR 2018 (IEI - ISHRAE). pp. 13-16.